

# THE EFFECT OF DIFFERENT OBSERVATIONAL DATA ON THE CONSTRAINTS OF COSMOLOGICAL PARAMETERS

YUNGUI GONG<sup>1,2,3</sup>, QING GAO<sup>2</sup>, AND ZONG-HONG ZHU<sup>4</sup>

*Draft version January 4, 2012*

## ABSTRACT

The constraints on  $\Lambda$ CDM model from type Ia supernova data alone and BAO data alone are similar, so it is worthwhile to compare their constraints on the property of dark energy. We use the SNLS3 compilation of 472 type Ia supernova data, the Gamma Ray Bursts data, the baryon acoustic oscillation measurement of distance, the cosmic microwave background radiation data from the seven year Wilkinson Microwave Anisotropy Probe, and the Hubble parameter data to study the effect of their different combinations on the fittings of cosmological parameters. Neither BAO nor WMAP7 data alone gives good constraint on the equation of state parameter of dark energy, but both WMAP7 data and BAO data help type Ia supernova data break the degeneracies among the model parameters, hence tighten the constraint on the variation of equation of state parameter  $w_a$ , and WMAP7 data does the job a little better. Although BAO and WMAP7 data provide reasonably good constraints on  $\Omega_m$  and  $\Omega_k$ , it is not able to constrain the dynamics of dark energy, we need SNe Ia data to probe the property of dark energy, especially the variation of the equation of state parameter of dark energy. The addition of  $H(z)$  data helps better constrain the geometry of the universe  $\Omega_k$  and the property of dark energy. For the SNLS SNe Ia data, the nuisance parameters  $\alpha$  and  $\beta$  are consistent for all different combinations of the above data. Their impacts on the fittings of cosmological parameters are minimal.  $\Lambda$ CDM model is consistent with all the observational data and it is favored against Dvali-Gabadadze-Porrati model.

*Subject headings:* cosmological parameters; dark energy

## 1. INTRODUCTION

The accelerating expansion of the universe was first discovered in 1998 by the observations of Type Ia supernovae (SNe Ia) (Riess et al. 1998; Perlmutter et al. 1999). As more accurate data are available, it is possible to measure the acceleration and the dynamical mechanism behind the acceleration. There are three different possibilities for the acceleration. The first possibility is that a new exotic form of matter with negative pressure, dubbed as dark energy drives the Universe to accelerate. The cosmological constant is the simplest candidate of dark energy which is also consistent with observations, but at odds with quantum field theory. The second possibility is that general relativity is modified at the cosmological scale, such as Dvali-Gabadadze-Porrati (DGP) model (Dvali, Gabadadze & Porrati 2000). The third possibility is that the universe is inhomogeneous. In this paper, we consider the possibility of dark energy only.

In the recent release of the measurements of the baryon acoustic oscillation (BAO) peaks at redshifts  $z = 0.44$ , 0.6 and 0.73 in the galaxy correlation function of the final dataset of the WiggleZ dark energy survey, Blake et al. (2011) used these three BAO data along with BAO data at redshifts  $z = 0.2$  and 0.35 measured from the

distribution of galaxies (Percival et al. 2010) and the measurement of BAO at redshift  $z = 0.106$  from the 6-degree Field Galaxy Survey (6dFGS) (Beutler et al. 2011) to constrain  $\Lambda$ CDM model. It was found that the constraints on  $\Lambda$ CDM model from BAO data only are even better than those from Union2 SNe Ia data (Amanullah et al. 2010) only. This means that the current BAO data is robust to constrain cosmological parameters. Because there are more than 500 SNe Ia data points, and only 6 data points in the updated BAO data, the fitting process for BAO data is easier and faster than that for SNe Ia data. If the constraints on the property of dark energy from BAO data are tighter than those from SNe Ia data, then we just need to apply BAO data only for a faster fitting although SNe Ia data and BAO data are complementary to each other. In this paper, we use a simple dark energy model to test the robustness of BAO data, and compare the constraints on the equation of state of dark energy from different data.

The geometry of the universe is sensitive to the cosmic microwave background (CMB) data, so it is expected that the addition of the seven-year Wilkinson Microwave Anisotropy Probe (WMAP7) data to either SNe Ia or BAO data helps tighten the constraints on  $\Lambda$ CDM model. Blake et al. (2011) found that the combination of BAO and WMAP7 data gives much better constraints on  $\Lambda$ CDM model than the combination of SNe Ia and WMAP7 data does. Sullivan et al. (2011) found that both SNLS3 SNe Ia data alone and the combination of WMAP7 and BAO data at redshifts  $z = 0.2$  and  $z = 0.35$  (Percival et al. 2010) gave similar constraint on the equation of state parameter  $w$  for the flat constant  $w$  model. The redshifts of BAO data span from  $z = 0.106$  to  $z = 0.73$ , we may expect that BAO data catches the

<sup>1</sup> School of Physics, Huazhong University of Science and Technology, Wuhan 430074, China

<sup>2</sup> College of Mathematics and Physics, Chongqing University of Posts and Telecommunications, Chongqing 400065, China; gongyg@cqupt.edu.cn

<sup>3</sup> Institute of Theoretical Physics, Chinese Academy of Sciences, Beijing 100190, China

<sup>4</sup> Department of Astronomy, Beijing Normal university, Beijing 100875, China; zhuzh@bnu.edu.cn

dynamical property of dark energy, so it is necessary to study the effects of different observational data and their combinations on the constraints on the equation of state of dark energy.

The question whether dark energy is just the cosmological constant remains to be answered. Recently, there are lots of studies in determining whether  $\Lambda$ CDM model is consistent with observations (Huang et al. 2009; Shafieloo, Sahni & Starobinsky 2009; Cai, Su & Zhang 2010; Lampeitl et al. 2009; Serra et al. 2009; Gong et al. 2010a; Gong, Wang & Cai 2010b; Pan et al. 2010; Gong, Zhu & Zhu 2011; Li et al. 2011). Li, Wu & Yu (2011) considered the tensions between different dataset through the reconstruction of  $Om(z)$  by using Chevallier-Polarski-Linder (CPL) parametrization (Chevallier & Polarski 2001; Linder 2003) of the equation of state of dark energy. They found that a tension between low redshift and high redshift data existed. Cai, Su & Tuo (2011) used the figure of merit (FOM) proposed by the Dark Energy Task Force (Albrecht et al. 2006) as a diagnostic to study the effectiveness of different combinations of data on constraining  $w_0$  and  $w_a$  in CPL model.

In this paper, we first study the robustness of BAO data, then study the constraints on the equation of state of dark energy based on different combinations of the following data: the three year Supernova Legacy Survey (SNLS3) sample of 472 SNe Ia data with systematic errors (Conley et al. 2011); the 59 Gamma Ray Bursts (GRB) data (Wei 2010); the BAO measurements from the 6dFGS (Beutler et al. 2011), the distribution of galaxies (Percival et al. 2010) and the WiggleZ dark energy survey (Blake et al. 2011); the WMAP7 data (Komatsu et al. 2011); and the Hubble parameter  $H(z)$  data (Gaztañaga, Cabré & Hui 2009b; Stern et al. 2010). In addition to studying the effects of different observational data and their combinations on the constraints of cosmological parameters, we also reconstruct the equation of state of dark energy  $w(z)$ , the deceleration parameter  $q(z)$  and  $Om(z)$  by using these datasets.

The paper is organized as follows. In section 2, we present the SNLS3 SNe Ia data (Conley et al. 2011), the GRB data (Wei 2010), the BAO data (Beutler et al. 2011; Blake et al. 2011; Percival et al. 2010), the WMAP7 data (Komatsu et al. 2011), the  $H(z)$  data (Gaztañaga, Cabré & Hui 2009b; Stern et al. 2010), and all the formulae related to these data. In section 3, we present all the models and the fitting results, and conclusions are drawn in section 4.

## 2. OBSERVATIONAL DATA

The SNLS3 SNe Ia data consists of 123 low-redshift SNe Ia data with  $z \lesssim 0.1$  mainly from Calan/Tololo, CfAI, CfAII, CfAIII and CSP, 242 SNe Ia over the redshift range  $0.08 < z < 1.06$  observed from the SNLS (Conley et al. 2011), 93 intermediate-redshift SNe Ia data with  $0.06 \lesssim z \lesssim 0.4$  observed during the first season of Sloan Digital Sky Survey (SDSS)-II supernova (SN) survey (Kessler et al. 2010), and 14 high-redshift SNe Ia data with  $z \gtrsim 0.8$  from Hubble Space Telescope (Riess et al. 2007). The SNLS3 SNe Ia data used the combination of SALT2 and SiFTO light-curve fitters (Conley et al. 2011). To use the 472 SNLS3 SNe Ia data

(Conley et al. 2011), we minimize

$$\chi_{sn}^2(\mathbf{p}, \alpha, \beta) = \sum_{i,j=1}^{472} (m_B - m_{mod})^T C_{sn}^{-1} (m_B - m_{mod}), \quad (1)$$

where  $m_B$  is the rest-frame peak B-band magnitude of a SN, the predicted magnitude of the SN given a cosmological model is  $m_{mod} = 5 \log_{10} \mathcal{D}_L(z_{hel}, z_{cmb}, \mathbf{p}) - \alpha(s - 1) + \beta\mathcal{C} + \mathcal{M}_B$ ,  $z_{hel}$  and  $z_{cmb}$  are the heliocentric and the CMB frame redshifts of the SN,  $s$  is the stretch given by the data,  $\mathcal{C}$  is the color measure for the SN given by the data,  $\alpha$  and  $\beta$  are nuisance parameters used for the SNLS3 data fitting,  $\mathcal{M}_B$  is another nuisance parameter incorporating the absolute magnitude and Hubble constant and it is marginalized over in the SN fitting process because of the arbitrary normalization of the magnitude,  $C_{sn}(z_i, z_j)$  is the covariant matrix which includes both the systematical and statistical uncertainties for the SNe Ia data (Conley et al. 2011). The correction on the dependence of the host-galaxy stellar mass is also included. The Hubble-constant free luminosity distance  $\mathcal{D}_L(z)$  is

$$\mathcal{D}_L(z) = H_0 d_L(z) = \frac{1+z}{\sqrt{|\Omega_k|}} S_k \left[ \sqrt{|\Omega_k|} \int_0^z \frac{dx}{E(x)} \right], \quad (2)$$

where the dimensionless Hubble parameter  $E(z) = H(z)/H_0$ , and  $S_k(x)$  is defined as  $x$ ,  $\sin(x)$  or  $\sinh(x)$  for  $k = 0, +1$ , or  $-1$ , respectively. For the fitting to the SNLS3 data, we need to add two more nuisance parameters  $\alpha$  and  $\beta$  in addition to the model parameters  $\mathbf{p}$  and the nuisance parameter  $\mathcal{M}_B$ .

The fitting of GRB data (Wei 2010) is similar to that of SNe Ia data except that the distance modulus  $\mu = m - \mathcal{M} = 5 \log_{10} \mathcal{D}_L(z, \mathbf{p})$  is used instead, so the fitting is simpler.

For the BAO data, we use the measurements from the 6dFGS (Beutler et al. 2011), the distribution of galaxies (Percival et al. 2010) and the WiggleZ dark energy survey (Blake et al. 2011). Percival et al. (2010) measured the distance ratio,

$$d_z = \frac{r_s(z_d)}{D_V(z)} \quad (3)$$

at two redshifts  $z = 0.2$  and  $z = 0.35$  to be  $d_{0.2}^{obs} = 0.1905 \pm 0.0061$ , and  $d_{0.35}^{obs} = 0.1097 \pm 0.0036$ . Here the effective distance is

$$D_V(z) = \left[ \frac{d_L^2(z)}{(1+z)^2} \frac{z}{H(z)} \right]^{1/3}, \quad (4)$$

$z_d$  is the drag redshift defined in Eisenstein & Hu (1998), the comoving sound horizon is

$$r_s(z) = \int_z^\infty \frac{c_s(x) dx}{E(x)}, \quad (5)$$

where the sound speed  $c_s(z) = 1/\sqrt{3[1 + \bar{R}_b/(1+z)]}$ , and  $\bar{R}_b = 3\Omega_b h^2/(4 \times 2.469 \times 10^{-5})$ . Beutler et al. (2011) derived that  $d_{0.106}^{obs} = 0.336 \pm 0.015$ . The WiggleZ dark energy survey measured the acoustic parameter

$$A(z) = \frac{D_V(z) \sqrt{\Omega_m H_0^2}}{z}, \quad (6)$$

at three redshifts  $z = 0.44$ ,  $z = 0.6$  and  $z = 0.73$ , and the results and their covariance matrix are listed in table 3 and table 2 in Blake et al. (2011). To use the BAO data, we minimize

$$\chi_{Bao}^2(\mathbf{p}, \Omega_b h^2, h) = \sum_{i,j=1}^2 \Delta d_i C_{dz}^{-1}(d_i, d_j) \Delta d_j + \frac{(d_{0.106} - 0.336)^2}{0.015^2} + \sum_{i,j=1}^3 \Delta A_i C_A^{-1}(A_i, A_j) \Delta A_j, \quad (7)$$

where  $d_i = (d_{z=0.2}, d_{z=0.35})$ ,  $\Delta d_i = d_i - d_i^{obs}$  and the covariance matrix  $C_{dz}(d_i, d_j)$  for  $d_z$  at  $z = (0.2, 0.35)$  is taken from equation (5) in Percival et al. (2010);  $A_i = (A(0.44), A(0.6), A(0.73))$ ,  $\Delta A_i = A(z_i) - A(z_i)^{obs}$  and the covariance matrix  $C_A(A_i, A_j)$  for the data points  $A(z)$  at  $z = (0.44, 0.6, 0.73)$  is taken from table 2 in Blake et al. (2011). Besides the model parameters  $\mathbf{p}$ , we need to add two more nuisance parameters  $\Omega_b h^2$  and  $\Omega_m h^2$  when we use the BAO data.

For the WMAP7 data, we use the measurements of the three derived quantities: the shift parameter  $R(z^*)$  and the acoustic index  $l_A(z^*)$  at the recombination redshift  $z^*$ . In particular, we minimize

$$\chi_{CMB}^2(\mathbf{p}, \Omega_b h^2, h) = \sum_{i,j=1}^3 \Delta x_i C_{CMB}^{-1}(x_i, x_j) \Delta x_j, \quad (8)$$

where the three parameters  $x_i = [R(z^*), l_A(z^*), z^*]$ ,  $\Delta x_i = x_i - x_i^{obs}$  and the covariance matrix  $C_{CMB}(x_i, x_j)$  for the three parameters is taken from Table 10 in Komatsu et al. (2011). The shift parameter  $R$  is expressed as

$$R(z^*) = \frac{\sqrt{\Omega_m} \mathcal{D}_L(z^*)}{1 + z^*} = 1.725 \pm 0.018. \quad (9)$$

The acoustic index  $l_A$  is

$$l_A(z^*) = \frac{\pi d_L(z^*)}{(1 + z^*) r_s(z^*)} = 302.09 \pm 0.76, \quad (10)$$

and  $z^*$  is the redshift at the recombination with the parametrization defined in Hu & Sugiyama (1996). We also need to add the nuisance parameters  $\Omega_b h^2$  and  $\Omega_m h^2$  to the parameter space when we employ the WMAP7 data.

Additionally, we use the  $H(z)$  data at 11 different redshifts obtained from the differential ages of red-envelope galaxies in Stern et al. (2010), and three more Hubble parameter data  $H(z = 0.24) = 76.69 \pm 2.32$ ,  $H(z = 0.34) = 83.8 \pm 2.96$  and  $H(z = 0.43) = 86.45 \pm 3.27$ , determined by Gaztañaga, Cabré & Hui (2009b). So we add these  $H(z)$  data to  $\chi^2$ ,

$$\chi_H^2(\mathbf{p}, h) = \sum_{i=1}^{14} \frac{[H(z_i) - H_{obs}(z_i)]^2}{\sigma_{hi}^2}, \quad (11)$$

where  $\sigma_{hi}$  is the  $1\sigma$  uncertainty of  $H(z)$ . Basically, the model parameters  $\mathbf{p}$  are determined by minimizing

$$\chi^2 = \chi_{sn}^2 + \chi_{grb}^2 + \chi_{Bao}^2 + \chi_{CMB}^2 + \chi_H^2. \quad (12)$$

The likelihood for the parameters  $\mathbf{p}$  in the model and the nuisance parameters is computed using the Monte Carlo Markov Chain (MCMC) method. The MCMC method randomly chooses values for the above parameters  $\mathbf{p}$ , evaluates  $\chi^2$  and determines whether to accept or reject the set of parameters  $\mathbf{p}$  using the Metropolis-Hastings algorithm. The set of parameters that are accepted to the chain forms a new starting point for the next process, and the process is repeated for a sufficient number of steps until the required convergence is reached. Our MCMC code is based on the publicly available package COSMOMC (Lewis & Bridle 2002; Gong, Wu & Wang 2008).

After fitting the observational data to different dark energy models, we apply the  $Om$  diagnostic (Sahni, Shafieloo & Starobinsky 2008) to detect the deviation from the  $\Lambda$ CDM model. For a flat universe (Sahni, Shafieloo & Starobinsky 2008),

$$Om(z) = \frac{E^2(z) - 1}{(1 + z)^3 - 1}. \quad (13)$$

For the flat  $\Lambda$ CDM model,  $Om(z) = \Omega_m$  is a constant which is independent of the value of  $\Omega_m$ . Because of this property,  $Om$  diagnostic is less sensitive to observational errors than the equation of state parameter  $w(z)$  does. On the other hand, the bigger the value of  $Om(z)$ , the bigger the value of  $w(z)$ , so the behavior of  $Om(z)$  catches the dynamical property of  $w(z)$ .

We also apply the FOM as a diagnostic tool to compare the effectiveness of different combinations of observational data on constraining the equation of state parameters  $w_0$  and  $w_a$  in CPL model. FOM is defined as the reciprocal of the area of the error ellipse enclosing the 95% confidence limit in the  $w_0$ - $w_a$  plane, it is proportional to  $[\det C_w(w_0, w_a)]^{-1/2}$ , here  $C_w(w_0, w_a)$  is the correlation matrix of  $w_0$  and  $w_a$ .

### 3. COSMOLOGICAL FITTING RESULTS

We first review the effects of different combinations of observational data on  $\Lambda$ CDM model. The  $\Omega_m$ - $\Omega_\Lambda$  contour for applying only the SNLS3 SNe data was shown in Figure 8 in Conley et al. (2011). By combining the SNLS3 SNe and the WMAP7 data, Sullivan et al. (2011) obtained the constraint on  $\Omega_m$  and  $\Omega_k$ , and  $\Omega_m$ - $\Omega_k$  contour was shown in Figure 4 of their paper. From these results, we see that SNLS3 SNe data alone does not provide tight constraint on  $\Omega_m$  and  $\Omega_k$ . With the addition of WMAP7 data, the constraint on  $\Omega_k$  becomes much tighter, henceforth tightens the constraint on  $\Omega_m$ . Therefore, WMAP7 data can be used to tighten the constraint on the geometry of the universe as shown in Figure 15 in Blake et al. (2011). In the same figure, Blake et al. (2011) showed the constraint on  $\Omega_m$  and  $\Omega_k$  by applying the BAO data only with the assumption that  $\Omega_b h^2 = 0.02227$ . Comparing the constraints from SNLS3 or Union2 SNe Ia data alone with that from BAO data alone, we see that the constraints are similar, and the constraint on  $\Omega_m$  is much better by using BAO data alone than that by using SNe Ia data alone. Blake et al. (2011) also compared the constraints on  $\Lambda$ CDM model by using the combination of BAO and Union2 SNe Ia data with the addition of WMAP7 data, and they found that  $\Omega_m$ - $\Omega_k$  contour became much smaller with the com-

combination of BAO and WMAP7 data compared with that using the combination of Union2 SNe Ia and WMAP7 data. Moreover, the constraint from the combination of Union2 SNe Ia, BAO and WMAP7 data is similar to that from BAO and WMAP7 data. These results show that BAO data mainly tightens the constraint on  $\Omega_m$  and WMAP7 data mainly tightens the constraint on  $\Omega_k$ , while current SNe Ia data still gave large  $\Omega_m$ - $\Omega_k$  contour. For comparison, we show all the constraints in Figure 1. Note that we set  $\Omega_b h^2$  as a free nuisance parameter. In Figure 1, we show the constraints on  $\Lambda$ CDM model from SNLS3 SNe Ia data alone (the green lines), BAO data alone (the yellow line), the combination of SNLS3 SNe Ia and BAO data (the cyan lines), the combination of SNLS3 SNe Ia and WMAP7 data (the magenta lines), the combination of BAO and WMAP7 data (the blue lines), the combination of SNLS3 SNe Ia, BAO and WMAP7 data (the red lines), the combination of SNLS3 SNe Ia, BAO, WMAP7 and  $H(z)$  data (the black lines), and the combination of SNLS3 SNe Ia, BAO, WMAP7, GRB and  $H(z)$  data (the shaded regions). As expected, GRB data has little effect on the  $\Omega_m$ - $\Omega_k$  contour when it is combined with the SNe Ia data. This point was also found in Cai, Su & Tuo (2011). In the following analysis, we do not consider the effect of GRB data alone on constraining cosmological parameters.  $H(z)$  data further reduces the errors on  $\Omega_k$  and moves the best fit value of  $\Omega_k$  toward zero. These results along with the constraints on the nuisance parameters  $\alpha$  and  $\beta$  are summarized in table 1. The error bars of  $\alpha$  and  $\beta$  are around 0.1, and they are consistent at  $1\sigma$  level for different fittings. The best fit value of  $\Omega_m$  from SNe Ia data is marginally consistent with that from BAO data, this shows a little tension between SN Ia and BAO data. The tension between BAO measurement and higher redshift type Ia supernova (SN Ia) was noticed in Percival et al. (2007), and the tension was lessened in Percival et al. (2010) due to revised error analysis, different methodology adopted and more data.

### 3.1. CPL parametrization

In this section, we apply the CPL parametrization (Chevallier & Polarski 2001; Linder 2003),

$$w(z) = w_0 + \frac{w_a z}{1+z}, \quad (14)$$

to test the effects of different combinations of data on constraining the property of dark energy. In this model, we have four model parameters  $\mathbf{p} = (\Omega_m, \Omega_k, w_0, w_a)$ . From the results of  $\Lambda$ CDM model, we know the constraints on  $\Omega_k$  from either SNe Ia data alone or BAO data alone are not good. For the curved CPL model, due to the addition of two more model parameters, we expect the situation becomes worse and in fact this is true. So we only consider the combinations of SNLS3 SNe Ia and/or BAO data with WMAP7 data. The contours are shown in figure 2 and the upper panels of figure 3. The  $1\sigma$  results along with the constraints on the nuisance parameters  $\alpha$  and  $\beta$  are summarized in table 2. As expected, we see that the constraint on  $\Omega_k$  from the combination of BAO and WMAP7 data (the blue lines) is better than that from the combination of SNe Ia and WMAP7 data (the magenta lines). The  $\Omega_m$ - $\Omega_k$  contour becomes much smaller when we combine SNe Ia, BAO and WMAP7 data (the red lines). The addition of  $H(z)$

further reduces the errors on  $\Omega_k$  and moves the best fit value of  $\Omega_k$  toward zero. From the  $w_0$ - $w_a$  contours in Figure 2, we see that the constraints from the combination of SNe Ia and WMAP7 data are much better than those from the combination of BAO and WMAP7 data, and the FOM is almost 5 times larger. The uncertainties in  $w_a$  from the combination of SNe Ia, BAO and WMAP7 data are reduced more than half compared with those from the combination of SNe Ia and WMAP7 data, the FOM increase more than 4 times. When SNe Ia data is combined with other data,  $\Omega_k$  is degenerated with  $w_0$  and  $w_a$ . As  $\Omega_k$  increases, the uncertainties in  $w_a$  reduced. However, for the combination of BAO and WMAP7 data, the degeneracies between  $\Omega_k$  and  $w_0$  and  $w_a$  become weaker. Therefore, although SNe Ia data does not provide tight constraints on  $\Omega_m$  and  $\Omega_k$ , its constraint on the equation of state parameter of dark energy is much better.  $\Lambda$ CDM model (the cross) is outside the  $1\sigma$  contour when we use the combination of SNe Ia, BAO and WMAP7 data (the red lines). With the addition of  $H(z)$  data, the  $w_0$ - $w_a$  contour is further reduced and  $\Lambda$ CDM model is inside the  $1\sigma$  contour. By using the constraints from the combination of all observational data, we reconstruct  $w(z)$  and the result is shown in figure 4.

Since WMAP7 data greatly reduces the error on  $\Omega_k$ , its effect on flat CPL model still needs to be studied. In Figure 4, we show the marginalized  $w_0$ - $w_a$  contour plots constrained from different combinations of data. The  $1\sigma$  results along with the constraints on the nuisance parameters  $\alpha$  and  $\beta$  are summarized in table 2. The constraints on  $w_0$  and  $w_a$  from BAO data alone are not good, so the results are not shown and BAO data alone is not discussed in the rest of this paper. The constraint from SNe Ia data alone is similar to that from the combination of SNe Ia and WMAP7 data in the curved case. This is easily understood because the addition of WMAP7 data in the curved case is used to limit the  $\Omega_k$  around zero. When the BAO data is added to the SNe Ia data, the uncertainty in  $w_a$  is reduced more than half and the FOM becomes 5 times larger. When WMAP7 data is added to the SNe Ia data, the uncertainty in  $w_a$  is reduced a little further and the FOM becomes almost 10 times larger. Compared with the constraint from the combination of BAO and WMAP7 data, we see that the SNe Ia data constrains better on  $w_0$  and the FOM is just one half smaller, both BAO and WMAP7 data help reduce the uncertainties in  $w_a$ , the help from WMAP7 data is a little better. When the combined SNe Ia, BAO and WMAP7 data are used, we get better constraints on  $w_0$  and  $w_a$ . The addition of GRB and  $H(z)$  further reduces the uncertainties in  $w_0$  and  $w_a$ . By using the constraints from the combination of all observational data, we reconstruct  $w(z)$  and  $Om(z)$  and the results are shown in figure 4.  $\Lambda$ CDM model is consistent with almost all the combinations of different data at  $1\sigma$  level.

From the above discussion, we find that WMAP7 data helps reduce the uncertainties in  $\Omega_k$  and BAO data helps reduce the uncertainties in  $\Omega_m$ . Neither BAO nor WMAP7 data alone gives good constraint on  $w_0$  and  $w_a$ , but both WMAP7 data and BAO data help SNe Ia data break the degeneracies among the model parameters, hence tighten the constraint on the variation of equation of state parameter  $w_a$ , and WMAP7 data does the job a little better. SNLS3 SNe Ia data alone does not

provide good constraints on  $\Omega_m$  and  $\Omega_k$ , but it provides good constraints on the parameters  $w_0$  and  $w_a$ , so it is necessary to apply SNe Ia data to probe the dynamical property of dark energy. The addition of  $H(z)$  data help better constrain the geometry of the universe  $\Omega_k$  and the property of dark energy. Due to the degeneracies among the model parameters, we need to measure  $\Omega_m$  and  $\Omega_k$  more precisely in order to better probe the property of dark energy. In other words, we need to combine different observational data such as SNe Ia, BAO, WMAP7 and  $H(z)$  data as long as the tensions among those data are not too big. The SNLS3 SNe Ia data fitting parameters  $\alpha$  and  $\beta$  are consistent at  $1\sigma$  level for different combinations of SNe Ia with other data.

### 3.2. Piecewise parametrization of $w(z)$

To see the property of dark energy constrained by current observational data, we apply all the observational data outlined in the previous section to the piecewise parametrization of  $w(z)$  for flat case,

$$\Omega_{DE}(z) = (1 - \Omega_m)(1 + z)^{3(1+w_N)} \prod_{i=1}^N (1 + z_{i-1})^{3(w_{i-1} - w_i)}, \quad (15)$$

where  $z_{i-1} \leq z < z_i$ ,  $z_0 = 0$ ,  $z_1 = 0.1$ ,  $z_2 = 0.4$ ,  $z_3 = 0.7$  and  $z_4 = 1.4$ . We also assume that  $w(z > 1.4) = -1$ . Following Huterer & Cooray (2005), we transform the parameters  $w_i$  to the de-correlated parameters  $\mathcal{W}_i$ . The results of  $\mathcal{W}_i$  are shown in the lower right panel of Figure 4. The results are similar with those using Union2 SNe Ia data (Amanullah et al. 2010) and previous BAO data (Gaztañaga, Miquel & Sánchez 2009a; Percival et al. 2010) in Gong, Zhu & Zhu (2011), and flat  $\Lambda$ CDM model is consistent with the observational data.

### 3.3. Modified holographic dark energy model

In addition to the model independent study, we consider a specific dark energy model in this subsection. Applying the relationship between the mass and the horizon of a Schwarzschild black hole in higher dimensions and holographic principle, a modified holographic dark energy model (MHDE) with Hubble horizon as the ultraviolet cutoff was proposed in Gong & Li (2010). Both DGP model (Dvali, Gabadadze & Porrati 2000) and  $\Lambda$ CDM model are special cases of this model. In this model, Friedmann equation is modified as (Gong & Li 2010; Dvali & Turner 2003)

$$E^2(z) - (1 - \Omega_m - \Omega_k - \Omega_r)E^{5-N}(z) = \Omega_k(1 + z)^2 + \Omega_m(1 + z)^3 + \Omega_r(1 + z)^4, \quad (16)$$

where  $N$  is the spatial dimension. So we recover the DGP model if  $N = 4$  and  $\Lambda$ CDM model if  $N = 5$ . This model has one more parameter than  $\Lambda$ CDM model, i.e., there are three parameters  $\mathbf{p} = (\Omega_m, \Omega_k, N)$  in this model. For the curved case,  $\Omega_k \neq 0$ , again we do not apply SNe Ia, BAO and WMAP7 data alone because the constraint is not expected to be good, but consider their combinations with WMAP7 data. The contours of  $\Omega_m$ - $\Omega_k$ ,  $\Omega_k$ - $N$ , and  $\Omega_m$ - $N$  are shown in Figure 5(a)-(c), and the  $1\sigma$  constraints are summarized in table 3. For the constraints on  $\Omega_m$  and  $\Omega_k$ , we see that the combination of BAO and WMAP7 data does better than the combination of SNe

Ia and WMAP7 data. However, for the constraint on  $N$ , both combinations get similar results. When we combine SNe Ia, BAO and WMAP7 data, the constraints on the model parameters  $\Omega_m$ ,  $\Omega_k$  and  $N$  are further improved. With the addition of GRB and  $H(z)$  data, the best fit value of  $\Omega_k$  is moved toward zero and the upper limit of  $N$  are reduced a little further. The results also show that observational data favors  $\Lambda$ CDM model more than DGP model since larger value of  $N$  is favored. The SNLS3 SNe Ia data fitting parameters  $\alpha$  and  $\beta$  are consistent for different data combinations.

For flat MHDE model, we consider the constraints from SNe Ia data, the combination of SNe Ia and BAO data, the combination of SNe Ia and WMAP7 data, the combination of BAO and WMAP7 data, the combination of SNe Ia, BAO and WMAP7 data, and the combinations of all the observational data, the contours of  $\Omega_m$ - $N$  are shown in Figure 5(d), and the  $1\sigma$  constraints are summarized in table 3. By setting  $\Omega_k = 0$ , as expected, the constraint on  $\Omega_m$  and  $N$  from SNe Ia data alone is similar to that from the combination of SNe Ia and WMAP7 data in curved case. With the addition of BAO data, the constraint on  $\Omega_m$  is improved greatly, hencefore improves the constraint on  $N$ . The effect of the combination of WMAP7 and SNe Ia data is similar to that of the combination of BAO and SNe Ia data except that the best fit values of the parameters  $\Omega_m$  and  $N$  become smaller. The effect of the combination of BAO and WMAP7 data is similar to that of the combination of SNe Ia and WMAP7 data except that the best fit value of  $\Omega_m$  becomes bigger and the best fit value of  $N$  becomes smaller. When we combine SNe Ia, BAO and WMAP7 data or all the observational data, the results are similar. For all the combinations,  $N \gtrsim 5$  at  $1\sigma$  level. The SNLS3 SNe Ia data fitting parameters  $\alpha$  and  $\beta$  are also consistent for different data combinations.

### 3.4. $q_1 - q_2$ parametrization

In this subsection, we reconstruct the deceleration parameter  $q(z)$  with a simple two-parameter function (Gong & Wang 2007),

$$q(z) = \frac{1}{2} + \frac{q_1 z + q_2}{(1 + z)^2}. \quad (17)$$

This parametrization recovers the matter dominated epoch at high redshift with  $q(z) = 1/2$ . The dimensionless Hubble parameter is

$$E(z) = \exp \left[ \int_0^z [1 + q(u)] d \ln(1 + u) \right] = (1 + z)^{3/2} \exp \left[ \frac{q_2}{2} + \frac{q_1 z^2 - q_2}{2(1 + z)^2} \right]. \quad (18)$$

Since  $E^2(z) \approx (1 + z)^3 \exp(q_1 + q_2)$  when  $z \gg 1$ , so the role of matter energy density is played by the sum of the two parameters,  $q_1 + q_2 = \ln \Omega_m$ . Although  $\Omega_m$  and  $\Omega_k$  are not model parameters in this parametrization, the comoving distance depends on  $\Omega_k$  through the function  $S_k$ , in order to better constrain the model parameters  $\mathbf{p} = (q_1, q_2)$ , we consider the flat case  $\Omega_k = 0$  only. As discussed above for the CPL model, the flat assumption of  $\Omega_k = 0$  may impose biased prior in the estimation of cosmological parameters due to the degeneracies among  $\Omega_m$ ,  $\Omega_k$  and  $w$  (Clarkson, Cortês & Bassett 2007). For this model, the only effect of  $\Omega_k$  is through  $S_k$ ,

and  $S_k(x) \approx x$  when  $\Omega_k$  is small, so the impact of the flat assumption is expected to be small. Fitting this model to SNe Ia data alone, we get the marginalized  $1\sigma$  constraints  $q_1 = -1.68^{+0.98}_{-0.87}$ ,  $q_2 = -1.06^{+0.19}_{-0.2}$ ,  $\alpha = 1.427^{+0.119}_{-0.096}$  and  $\beta = 3.262^{+0.118}_{-0.101}$ . The contour plot is shown in Figure 6(a). Using these results, we reconstruct  $q(z)$  and  $Om(z)$  and the results are shown in Figures 6(b) and 6(c). So  $q(z) < 0$  when  $z \lesssim 0.5$  at  $2\sigma$  level and flat  $\Lambda$ CDM model is consistent with the model at  $1\sigma$  level. With the SNe Ia data alone, the evidence for current acceleration and past deceleration is very strong.

When we fit the model to BAO or WMAP7 data, we need to include the radiation-dominated era, and the nuisance parameters  $\Omega_b h^2$  and  $\Omega_m h^2$  which are just data fitting parameters, so we do not apply BAO and WMAP7 data alone. For approximation, we take the following Hubble parameter,

$$E^2(z) = \Omega_r(1+z)^4 + (1+z)^3 \exp \left[ q_2 + \frac{q_1 z^2 - q_2}{(1+z)^2} \right], \quad (19)$$

where the current radiation component  $\Omega_r = 4.1736 \times 10^{-5} h^{-2}$  (Komatsu et al. 2011). Fitting the model to the combined SNe Ia, GRB, BAO, WMAP7 and  $H(z)$  data, we get the marginalized  $1\sigma$  constraints,  $q_1 = 0.18^{+0.14}_{-0.12}$  and  $q_2 = -1.45 \pm 0.1$ ,  $\alpha = 1.423^{+0.119}_{-0.096}$  and  $\beta = 3.262^{+0.115}_{-0.103}$ . The contour plot is shown in Fig. 6(a). Compared this result with that obtained from SNe Ia data alone, we find that they are inconsistent at  $1\sigma$  model, this shows the tension between SNe Ia, BAO and WMAP7 data in fitting this model. Using the  $q_1$ - $q_2$  contour, we reconstruct  $q(z)$  and  $Om(z)$  and the results are shown in Figures 6(b) and 6(c). We find that  $q(z)$  increases with the redshift and  $q(z) < 0$  when  $z \lesssim 0.5$  at  $2\sigma$  level, flat  $\Lambda$ CDM model is inconsistent with the model at  $2\sigma$  level. These results may suggest that the approximation (19) is not good at high redshift. Since  $\Omega_m$  does not appear in this model, it may not be straightforward to apply BAO and WMAP7 data, this needs to be further studied.

### 3.5. Piecewise parametrization of $q(z)$

We also apply the piecewise parametrization to study the property of the deceleration parameter  $q(z)$ . For  $z_{i-1} \leq z < z_i$ , we have

$$E(z) = (1+z)^{1+q_N} \prod_{i=1}^N (1+z_{i-1})^{q_{i-1}-q_i}. \quad (20)$$

In this model, we have four parameters  $\mathbf{p} = (q_1, q_2, q_3, q_4)$ . We think this model approximates the behavior of  $E(z)$  in the redshift range  $z \lesssim 1.5$ . In the radiation dominated era, we add the radiation contribution also. Again we follow Huterer & Cooray (2005) to transform the correlated parameters  $q_i$  to uncorrelated ones. Fitting the model to all observational data, we reconstruct the evolution of  $q(z)$  and the results are shown in Fig. 6(d). Similar to that obtained by Union2 SNe Ia data (Gong, Zhu & Zhu 2011), we find that  $q(z) < 0$  when  $z \lesssim 0.6$  and  $q(z) > 0$  at high redshift, so the evidences for current acceleration and past deceleration are very strong.

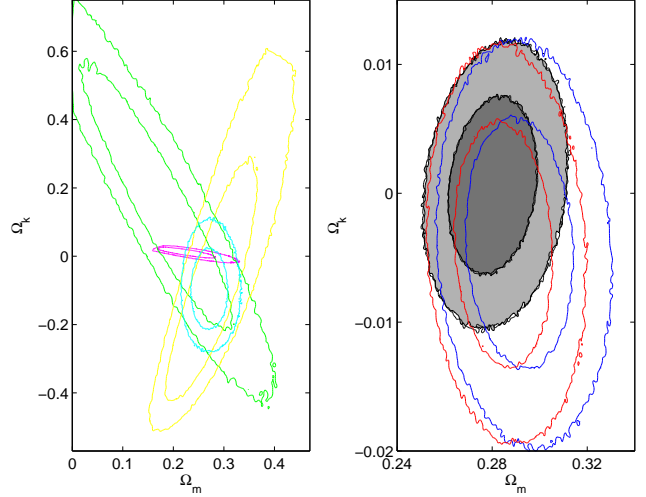


**Figure 1.** The marginalized  $1\sigma$  and  $2\sigma$  contour plots of  $\Omega_m$  and  $\Omega_k$  for the  $\Lambda$ CDM model. The green lines label the constraints from SNe Ia data only, the yellow lines label the constraints from BAO data only, the cyan lines label the constraints from the combination of SNe Ia and BAO data, the magenta lines label the constraints from the combination of SNe Ia and WMAP7 data, the blue lines label the constraints from the combination of WMAP7 and BAO data, the red lines label the constraints from the combination of SNe Ia, BAO and WMAP7 data, the black lines label the constraints from the combination of SNe Ia, BAO, WMAP7 and  $H(z)$  data, and the shaded regions label the constraints from the combination of all the observational data described in section 2.

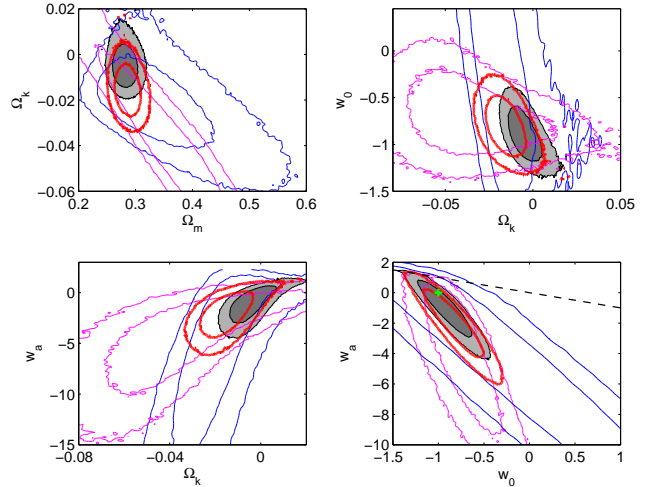


**Figure 2.** The marginalized  $1\sigma$  and  $2\sigma$  contour plots for the curved CPL model. The meaning of different colors is the same as that in Figure 1. The dashed line in the  $w_0$ - $w_a$  contour denotes the condition  $w_0 + w_a = 0$ . The + sign denotes the point corresponding to the  $\Lambda$ CDM model.

## 4. CONCLUSIONS

It is well known that BAO data is more sensitive to  $\Omega_m$  and WMAP7 data is more sensitive to  $\Omega_k$ . As more data points become available and the data becomes more accurate, we are able to constrain the cosmological parameters better. The constraints on  $\Lambda$ CDM model from SNLS3 SNe Ia data alone are similar to that from BAO data alone as shown in figure 1, so we may wonder if we can use BAO data alone to constrain the property of dark energy. Applying BAO data to CPL model and MHDE model, we find that the constraints on the dy-

**Table 1**The marginalized  $1\sigma$  errors for  $\Omega_m$  and  $\Omega_k$  in  $\Lambda$ CDM model constrained by different observational data

Data	$\Omega_m$	$\Omega_k$	$\alpha$	$\beta$
SNe Ia	$0.17^{+0.1}_{-0.09}$	$0.15 \pm 0.25$	$1.423^{+0.122}_{-0.094}$	$3.267^{+0.112}_{-0.109}$
BAO	$0.26^{+0.09}_{-0.03}$	$-0.16^{+0.38}_{-0.11}$		
SNe+BAO	$0.27 \pm 0.02$	$-0.11^{+0.09}_{-0.07}$	$1.428^{+0.114}_{-0.102}$	$3.249^{+0.125}_{-0.095}$
SNe+WMAP7	$0.22^{+0.05}_{-0.03}$	$0.01 \pm 0.01$	$1.422^{+0.121}_{-0.095}$	$3.26^{+0.115}_{-0.106}$
BAO+WMAP7	$0.29^{+0.02}_{-0.01}$	$-0.004^{+0.007}_{-0.006}$		
SNe+BAO+WMAP7	$0.28 \pm 0.01$	$-0.004^{+0.006}_{-0.007}$	$1.41^{+0.127}_{-0.088}$	$3.261^{+0.104}_{-0.116}$
SNe+BAO+WMAP7+ $H(z)$	$0.28^{+0.02}_{-0.01}$	$0.0006^{+0.0046}_{-0.0045}$	$1.429^{+0.108}_{-0.107}$	$3.245^{+0.120}_{-0.099}$
All	$0.28 \pm 0.01$	$0.0008^{+0.0043}_{-0.0048}$	$1.421^{+0.117}_{-0.098}$	$3.243^{+0.122}_{-0.098}$

**Table 2**The marginalized  $1\sigma$  constraints on CPL model by different observational data

Data	$\Omega_m$	$\Omega_k$	$w_0$	$w_a$	$\alpha$	$\beta$	FoM
BAO+WMAP7	$0.35 \pm 0.07$	$-0.023 \pm 0.013$	$0.4 \pm 1.4$	$-8.6^{+7.4}_{-7.2}$			0.36
SNe+WMAP7	$0.33^{+0.09}_{-0.06}$	$-0.03^{+0.02}_{-0.03}$	$-0.8^{+0.3}_{-0.2}$	$-3.4^{+2.1}_{-5.0}$	$1.430^{+0.111}_{-0.106}$	$3.262^{+0.117}_{-0.104}$	1.67
SNe+BAO+WMAP7	$0.28^{+0.02}_{-0.01}$	$-0.015^{+0.007}_{-0.008}$	$-0.8 \pm 0.2$	$-2.02^{+1.35}_{-1.66}$	$1.410^{+0.133}_{-0.082}$	$3.245^{+0.137}_{-0.084}$	7.29
All	$0.28^{+0.02}_{-0.01}$	$-0.004^{+0.006}_{-0.007}$	$-0.96^{+0.26}_{-0.13}$	$-0.66^{+0.72}_{-1.77}$	$1.4342^{+0.109}_{-0.107}$	$3.256^{+0.119}_{-0.102}$	9.73
SNe	$0.31^{+0.09}_{-0.07}$		$-0.8^{+0.4}_{-0.2}$	$-3.1^{+2.4}_{-5.9}$	$1.432^{+0.109}_{-0.107}$	$3.255^{+0.123}_{-0.099}$	1.15
SNe+BAO	$0.28^{+0.03}_{-0.02}$		$-0.83^{+0.26}_{-0.19}$	$-2.11^{+1.27}_{-1.95}$	$1.418^{+0.126}_{-0.090}$	$3.275^{+0.110}_{-0.112}$	5.94
SNe+WMAP7	$0.24^{+0.03}_{-0.02}$		$-0.9 \pm 0.2$	$-1.1^{+0.8}_{-1.4}$	$1.413^{+0.133}_{-0.083}$	$3.284^{+0.1}_{-0.122}$	10.39
BAO+WMAP7	$0.30 \pm 0.04$		$-0.81^{+0.58}_{-0.59}$	$-0.90^{+1.96}_{-1.91}$			2.38
SNe+BAO+WMAP7	$0.28^{+0.02}_{-0.01}$		$-1.12^{+0.27}_{-0.07}$	$0.32^{+0.21}_{-1.63}$	$1.429^{+0.112}_{-0.103}$	$3.261^{+0.111}_{-0.109}$	12.52
ALL	$0.28^{+0.02}_{-0.01}$		$-1.02^{+0.18}_{-0.11}$	$-0.20^{+0.39}_{-1.15}$	$1.416^{+0.125}_{-0.091}$	$3.246^{+0.125}_{-0.095}$	15.16

**Table 3**The marginalized  $1\sigma$  constraints on MHDE model by different observational data

Data	$\Omega_m$	$\Omega_k$	$N$	$\alpha$	$\beta$
BAO+WMAP7	$0.28 \pm 0.02$	$-0.01 \pm 0.01$	$6.0^{+2.5}_{-1.0}$		
SNe+WMAP7	$0.29^{+0.07}_{-0.08}$	$-0.02 \pm 0.03$	$6.5^{+1.7}_{-1.5}$	$1.434 \pm 0.108$	$3.268 \pm 0.11$
SNe+BAO+WMAP7	$0.28^{+0.02}_{-0.01}$	$-0.011 \pm 0.007$	$5.8^{+1.0}_{-0.8}$	$1.415^{+0.128}_{-0.088}$	$3.246^{+0.132}_{-0.088}$
All	$0.28 \pm 0.01$	$-0.001^{+0.004}_{-0.006}$	$5.3^{+0.8}_{-0.3}$	$1.415^{+0.126}_{-0.090}$	$3.251^{+0.122}_{-0.098}$
SNe	$0.26 \pm 0.09$		$6.1^{+2.0}_{-1.8}$	$1.435 \pm 0.108$	$3.268 \pm 0.11$
SNe+BAO	$0.28^{+0.02}_{-0.03}$		$5.8^{+1.2}_{-0.5}$	$1.432^{+0.112}_{-0.104}$	$3.254^{+0.126}_{-0.095}$
SNe+WMAP7	$0.25^{+0.03}_{-0.02}$		$5.3^{+0.8}_{-0.3}$	$1.434^{+0.11}_{-0.106}$	$3.259^{+0.12}_{-0.1}$
BAO+WMAP7	$0.29 \pm 0.02$		$4.9^{+0.8}_{-0.3}$		
SNe+BAO+WMAP7	$0.28 \pm 0.01$		$5.3^{+0.6}_{-0.3}$	$1.423^{+0.118}_{-0.098}$	$3.264^{+0.106}_{-0.114}$
All	$0.28 \pm 0.01$		$5.3^{+0.6}_{-0.2}$	$1.415^{+0.125}_{-0.09}$	$3.254^{+0.115}_{-0.09}$

namical behavior of dark energy from BAO data alone are much worse than those from SNe Ia data alone. Although SNe Ia data alone is not able to provide good constraints on  $\Omega_m$  and  $\Omega_k$ , it provides much better constraint on the equation of state parameter of dark energy compared with that from BAO and WMAP7 data alone. Since the way that the model parameters are degenerated is different for SNe Ia, BAO and WMAP7 data alone, it is a good idea to combine different dataset to get better constraint on the property of dark energy.

For the curved CPL model, we find that the combination of BAO and WMAP7 data gives better constraints on  $\Omega_m$  and  $\Omega_k$  than those from the combination of SNe Ia and WMAP7, but the constraints on  $w_0$  and  $w_a$  from the combination of BAO and WMAP7 data are much worse than those from the combination of SNe Ia and WMAP7

data. The variation of the equation of state parameter  $w_a$  is reduced more than half when we add BAO data to the combination of SNe Ia and WMAP7 data, and the FOM increases more than 4 times. The variation of the equation of state parameter  $w_a$  is reduced more than 5 times when we add SNe Ia data to the combination of BAO and WMAP7 data, and the FOM increases more than 20 times. Both WMAP7 data and BAO data help SNe Ia data break the degeneracies among the model parameters, hence tighten the constraint on the variation of equation of state parameter  $w_a$ , and WMAP7 data does the job a little better. GRB data has little effect on the constraints when it is combined with SNe Ia data.  $H(z)$  data helps move the best fit value of  $\Omega_k$  toward zero and make the model more compatible with  $\Lambda$ CDM model.

For the flat CPL model, we get similar constraints on



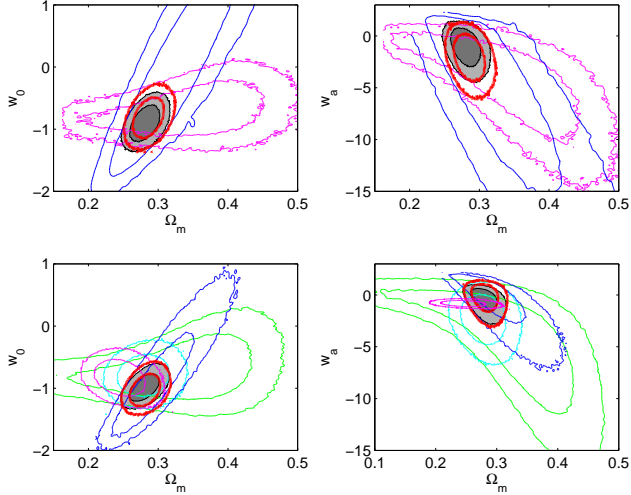


**Figure 3.** The marginalized  $1\sigma$  and  $2\sigma$  contour plots of  $\Omega_m$ - $w_0$  and  $\Omega_m$ - $w_a$  for the CPL model. The upper panels are for the curved case and the lower panels are for the flat case. The meaning of different colors is the same as that in Figure 1.

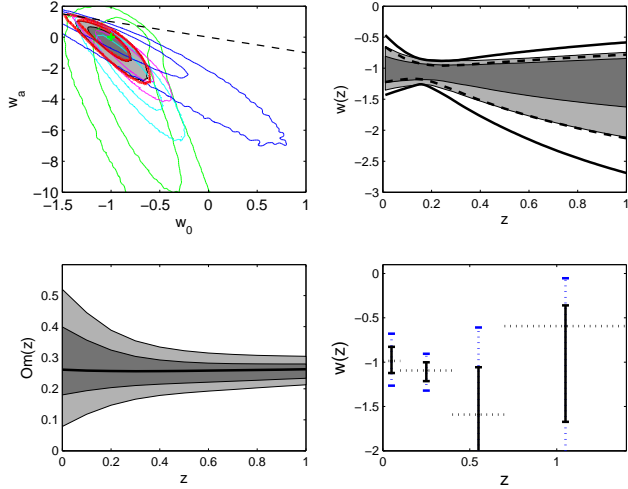


**Figure 4.** The marginalized  $1\sigma$  and  $2\sigma$  constraints from observations. In the upper left panel, we show the  $w_0$  and  $w_a$  contours for the flat CPL model from SNe Ia data alone (the green lines), the combination of SNe Ia and BAO data (the cyan lines), the combination of SNe Ia and WMAP7 data (the magenta lines), the combination of BAO and WMAP7 data (the blue lines), the combination of SNe Ia, BAO and WMAP7 data (the red lines), and the combination of all data (the shaded regions). The dashed line in the  $w_0$ - $w_a$  contour denotes the condition  $w_0 + w_a = 0$ . The + sign denotes the point corresponding to the  $\Lambda$ CDM model. In the upper right panel, we reconstruct the evolution of  $w(z)$  by using the constraints from the combination of all data for CPL model, the shaded regions are for flat CPL model, and the black lines are for curved CPL model. In the lower left panel, we reconstruct  $Om(z)$  by using the constraints from the combination of all data for flat CPL model, the solid line is obtained by using the best fitting values of  $\Omega_m$ ,  $w_0$  and  $w_a$ . In the lower right panel, we show the observational constraints on  $w(z)$  by using the piecewise parametrization.

$w_0$  and  $w_a$  for SNe Ia data alone and the combination of BAO and WMAP7 data. Replacing the SNe Ia data by the combination of BAO and WMAP7 data, the FOM is just doubled. When the BAO data is added to the SNe Ia data, the uncertainty in  $w_a$  is reduced more than half and the FOM becomes 5 times larger. When WMAP7 data is added to the SNe Ia data, the uncertainty in  $w_a$  is

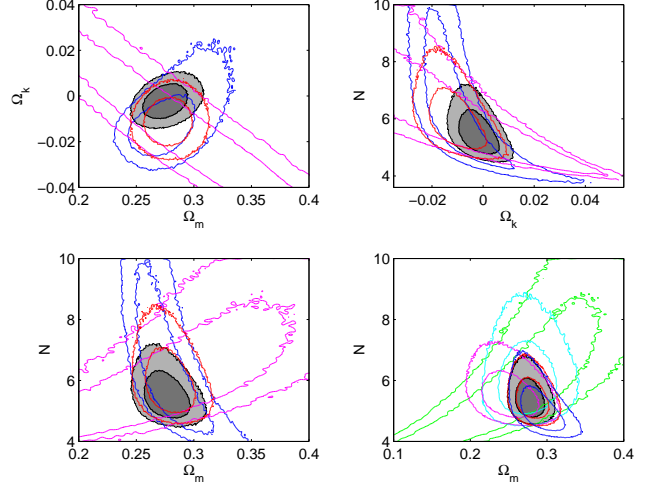


**Figure 5.** The marginalized  $1\sigma$  and  $2\sigma$  contour plots for MHDE model. The figures from the upper left to lower right are labeled as (a)-(d), respectively. (a)-(c) are for the curved MHDE model and (d) is for the flat MHDE model. The meaning of different colors is the same as that in Figure 1.

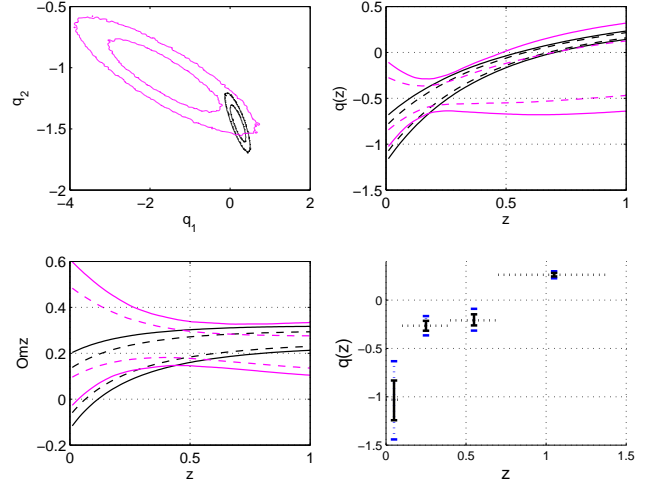


**Figure 6.** The marginalized  $1\sigma$  and  $2\sigma$  constraints on  $q_1$ - $q_2$  parametrization and the piecewise parametrization of  $q(z)$ , the magenta lines represent the results obtained from SNe Ia data alone and the black lines represent the results obtained from all the observational data. The figures from upper left to lower right are labeled as (a)-(d), respectively. (a) shows the contour plots for  $q_1$  and  $q_2$ , (b) and (c) show the reconstruction of  $q(z)$  and  $Om(z)$ , (d) shows the results for the piecewise parametrization of  $q(z)$  constrained by all the observational data.

reduced a little further and the FOM becomes almost 10 times larger. Both BAO and WMAP7 data help reduce the uncertainties in  $w_a$ , the help from WMAP7 data is a little better.  $\Lambda$ CDM model is consistent with all the observational data. This point is further supported by the reconstruction of  $w(z)$  and  $Om(z)$  as shown in Figure 4. For the MHDE model, we find that the constraints on  $N$  are similar for the combination of SNe Ia and BAO data, SNe Ia and WMAP7 data, and BAO and WMAP7 data. We also find that  $\Lambda$ CDM model is favored against DGP model.

To study the acceleration of the expansion of the universe, we reconstruct the deceleration parameter  $q(z)$  with a simple two-parameter function and the piecewise



parametrization which approximates the evolution of the universe in the redshift  $z \lesssim 1.5$ . For the SNe Ia data only, we see strong evidence that  $q(z) < 0$  in the redshift  $z \lesssim 0.5$ . The  $1\sigma$  contour from SNe Ia data only is inconsistent with that from the combination of all data, it seems that there exists some tensions between SNe Ia data and other data, however the inconsistency may come from the approximation we made at high redshift or the way we apply the BAO and WMAP7 data. Note that the usual model parameters  $\Omega_m h^2$  and  $\Omega_b h^2$  do not appear in the  $q(z)$  models, and BAO and WMAP7 data depend on those parameters, so we may not apply the BAO and WMAP7 data as usual, this needs to be further studied.

Although BAO and WMAP7 data provide reasonably good constraints on  $\Omega_m$  and  $\Omega_k$ , it is not able to constrain the dynamics of dark energy, we need SNe Ia data to probe the property of dark energy, especially the variation of the equation of state parameter of dark energy. The addition of BAO data helps reduce the error on  $\Omega_m$  and the addition of CMB data helps reduce the error on  $\Omega_k$ , so both BAO and CMB data help SNe Ia data tighten the constraints on the equation of state of dark energy due to degeneracies among  $\Omega_m$ ,  $\Omega_k$  and  $w(z)$ , but neither data alone can be used to probe the dynamical property of dark energy. For the SNLS SNe Ia data, the nuisance parameters  $\alpha$  and  $\beta$  are consistent for all different combinations of data. Their impacts on the fitting of cosmological parameters are minimal.

This work was partially supported by the National Basic Science Program (Project 973) of China under grant Nos. 2007CB815401 and 2010CB833004, the NNSF of China under grant Nos. 10935013 and 11175270, the Project of Knowledge Innovation Program (PKIP) of Chinese Academy of Sciences, Grant No. KJCX2.YW.W10, CQ CSTC under grant No. 2009BA4050 and CQ CMEC under grant No. KJTD201016. Z-HZ was partially supported by the NNSF Distinguished Young Scholar project under Grant No. 10825313.

## REFERENCES

- Albrecht, A. et al. 2006, arXiv: astro-ph/0609591  
Amanullah, R. et al. 2010, ApJ, 716, 712  
Beutler, F. et al. 2010, MNRAS, arXiv: 1106.3366.  
Blake, C. et al. 2011, arXiv: 1108.2635.  
Cai, R. G., Su, Q. P., & Zhang, H.-B. 2010, J. Cosm. Astropart. Phys., JCAP04(2010)012  
Cai, R. G., Su, Q. P., & Tuo, Z.-L. 2011, arXiv: 1109.2846.  
Chevallier, M., Polarski, D. 2001, Int. J. Mod. Phys. D, 10, 213  
Clarkson, C., Cortès, M., & Bassett, B. 2007, J. Cosm. Astropart. Phys., JCAP08(2007)011  
Conley, A. et al. 2011, arXiv: 1104.1443  
Dvali, G., Gabadadze, G., & Porrati, M. 2000, Phys. Lett. B, 485, 208  
Dvali, G., & Turner, M. S. 2003, arXiv: astro-ph/0301510  
Eisenstein, D. J., & Hu, W. 1998, ApJ, 496, 605  
Gaztañaga E., Miquel, R., & Sánchez, E. 2009a, Phys. Rev. Lett., 103, 091302  
Gaztañaga E., Cabré, A., & Hui, L. 2009b, MNRAS, 399, 1663  
Gong, Y. G., Wang, & A. 2007, Phys. Rev. D, 75, 043520  
Gong, Y. G., Wu, Q., & Wang, A. 2008, ApJ, 681, 27  
Gong, Y. G., & Li, T. J. 2010, Phys. Lett. B, 683, 241  
Gong, Y. G., Cai, R. G., Chen, Y., & Zhu, Z.-H. 2010a, J. Cosm. Astropart. Phys., JCAP01(2010)019  
Gong, Y. G., Wang, B., & Cai, R. G. 2010b, J. Cosm. Astropart. Phys., JCAP04(2010)019  
Gong, Y. G., Zhu, X. M., & Zhu, Z.-H. 2011, MNRAS, 415, 1943  
Hu, W., & Sugiyama, N. 1996, ApJ, 471, 542  
Huang, Q. G., Li, M., Li, X. D., & Wang, S. 2009, Phys. Rev. D, 80, 083515  
Huterer, D., & Cooray, A. 2005, Phys. Rev. D, 71, 023506  
Kessler, R. et al. 2010, ApJS, 185, 32  
Komatsu, E. et al. 2011, ApJS, 192, 18  
Lampeitl, H. et al. 2009, MNRAS, 401, 2331  
Lewis, A., & Bridle, S. 2002, Phys. Rev. D, 66, 103511  
Li, X.-D. et al. 2011, arXiv: 1106.4116  
Li, Z. X., Wu, P. X., & Yu, H. W. 2011, Phys. Lett. B, 695, 1  
Linder, E. V. 2003, Phys. Rev. Lett., 90, 091301  
Pan, N. N., Gong, Y. G., Chen, Y., & Zhu, Z.-H. 2010, Class. Quantum Grav., 27, 155015  
Percival, W. J. et al. 2007, MNRAS, 381, 1053  
Percival, W. J. et al. 2010, MNRAS, 401, 2148  
Perlmutter, S. et al. 1999, ApJ, 517, 565  
Riess, A. G. et al. 1998, AJ, 116, 1009  
Riess, A. G. et al. 2007, ApJ, 659, 98  
Sahni, V., Shafieloo, A., & Starobinsky, A. A. 2008, Phys. Rev. D, 78, 103502  
Serra, P., Cooray, A., Holz, D. E., Melchiorri, A., Pandolfi, S., & Sarkar, D. 2009, Phys. Rev. D, 80, 121302  
Shafieloo, A., Sahni, V., Starobinsky, & A., A. 2009, Phys. Rev. D, 80, 101301  
Stern, D., Jimenez, R., Verde, L., Kamionkowski, M., & Stanford, S. A. 2010, J. Cosm. Astropart. Phys., JCAP02(2010)008  
Sullivan, M. et al. arXiv: 1104.1444  
Wei, H. 2010, J. Cosm. Astropart. Phys., JCAP08(2010)020